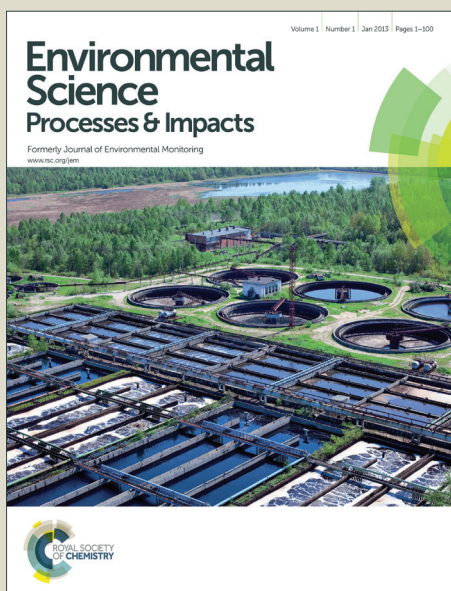


Environmental Science Processes & Impacts

Accepted Manuscript



This is an *Accepted Manuscript*, which has been through the Royal Society of Chemistry peer review process and has been accepted for publication.

Accepted Manuscripts are published online shortly after acceptance, before technical editing, formatting and proof reading. Using this free service, authors can make their results available to the community, in citable form, before we publish the edited article. We will replace this *Accepted Manuscript* with the edited and formatted *Advance Article* as soon as it is available.

You can find more information about *Accepted Manuscripts* in the [Information for Authors](#).

Please note that technical editing may introduce minor changes to the text and/or graphics, which may alter content. The journal's standard [Terms & Conditions](#) and the [Ethical guidelines](#) still apply. In no event shall the Royal Society of Chemistry be held responsible for any errors or omissions in this *Accepted Manuscript* or any consequences arising from the use of any information it contains.

Direct Photodegradation of Lamotrigine (an Antiepileptic) in Simulated Sunlight – pH Influenced Rates and Products

Robert B. Young[†], Benny Chefetz[‡], Aiju Liu[§], Yury Desyaterik[¶], and Thomas Borch^{†||*}

[†] Department of Soil and Crop Sciences, Colorado State University, Fort Collins, Colorado 80523-1170 United States

[‡] Department of Soil and Water Sciences, The Hebrew University of Jerusalem, P.O. Box 12, Rehovot 76100, Israel

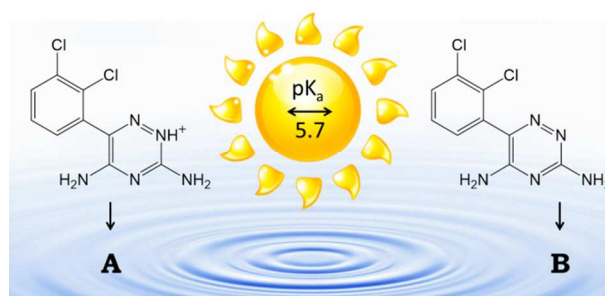
[§] School of Resources and Environmental Engineering, Shandong University of Technology, 12 Zhangzhou Road, Zibo, Shandong Province 255049 PR China

[¶] Department of Atmospheric Sciences, Colorado State University, Fort Collins, Colorado 80523-1371 United States

^{||} Department of Chemistry, Colorado State University, Fort Collins, Colorado 80523-1872 United States

TABLE OF CONTENTS

In simulated sunlight, pH influenced the direct photodegradation of lamotrigine, an antiepileptic drug recently detected in surface and drinking waters, producing different degradation rates, quantum yields, pathways, and photoproducts.



ENVIRONMENTAL IMPACT

The photochemical behavior of lamotrigine was studied in simulated sunlight, and buffered aqueous solutions at pH 3.3 (99.6% protonated), pH 5.3 (71.5% protonated) and pH 7.7 (1% protonated) were used to examine the influence of pH and protonation state on lamotrigine's molar absorptivity, photodegradation rate, reaction quantum yield, and photoproducts. This study provides insight into the photochemical fate of lamotrigine and its photoproducts in natural waters (pH 6 to 9), and tentatively identifies pH-dependent reaction mechanisms that may interact with natural water constituents like dissolved organic matter.

ABSTRACT

Lamotrigine is an antiepileptic and mood stabilizing drug that has been detected in wastewater, groundwater, surface water and drinking water, at frequencies in surface water ranging from 47 to 97%. Because lamotrigine is a weak base ($pK_a = 5.7$) that appears in two protonation states in natural waters, this study examined the direct photodegradation of lamotrigine (11.4 to 12.0 mg L⁻¹) in simulated sunlight using liquid chromatography- UV diode array detection and

buffered aqueous solutions at pH 3.3, 5.3, and 7.7. Lamotrigine's half-life varied little (100 ± 3 to 112 ± 2 h) with solution pH, but its specific light absorption rate was 12 times higher, and its reaction quantum yield was 13 times lower, at pH 7.7 versus pH 3.3. In the estimated midday, midsummer sunlight in Denver, CO, USA (latitude 39.8617°N), lamotrigine's estimated photodegradation rate was more than twice as fast at pH 7.7 versus pH 3.3. Lamotrigine's photoproducts were detected by liquid chromatography-UV diode array detection and time-of-flight mass spectrometry. Solution pH was shown to affect the identities and relative abundances of lamotrigine's photoproducts. Some photoproducts appeared only in solutions containing protonated lamotrigine, and others appeared only in solutions containing neutral lamotrigine. As a result, different reaction mechanisms were proposed. Finally, lamotrigine's reaction quantum yield ($2.51 \pm 0.07 \times 10^{-5}$ mol einstein⁻¹ at pH 7.7) and other results suggested that lamotrigine and three photoproducts are approximately as resistant to direct photodegradation as carbamazepine, a frequently detected pharmaceutical in surface waters.

INTRODUCTION

Due to their widespread use, incomplete removal during water treatment, and sensitive analytical techniques, trace quantities of pharmaceuticals and their metabolites have been detected in surface waters, groundwater, drinking water, soils, and biota throughout the world¹⁻⁴. As of the end of 2011, antiepileptics were the tenth most prescribed therapeutic class of pharmaceuticals in the United States (128 million prescriptions), and the 12th highest selling therapeutic class globally (US \$14.1 billion)^{5, 6}. A recent study synthesized 155 studies on pharmaceutical occurrence in freshwater ecosystems, covering the detection of 203 pharmaceuticals in surface waters across 41 countries, and determined that one epileptic drug, carbamazepine (CBZ), was the most frequently studied and detected compound in North America and Europe, and third in Asia¹. Two other antiepileptics (gabapentin and primidone) were among the 61 most frequently studied pharmaceuticals in surface waters, and among those with mean detection frequencies exceeding 75% (12 of 61)¹. In addition, two antiepileptic drugs (CBZ and phenytoin) have been among the most frequently detected pharmaceuticals in drinking water^{2, 7, 8}. Together, these data suggest that antiepileptics are ubiquitous in surface waters, and more recalcitrant than many other therapeutic classes of drugs.

Lamotrigine [3,5-diamino-6-(2,3-dichlorophenyl)-1,2,4-triazine] (LTG) is an antiepileptic and mood stabilizing drug marketed as Lamictal. In 2008, when generic lamotrigine tablets were introduced to the United States, Lamictal was the 19th highest selling brand name pharmaceutical (US \$1.5 billion)⁹. As an antiepileptic, LTG appears to be effective at treating primary generalized tonic-clonic seizures and absence seizures, and is at least as effective as CBZ, the standard drug treatment, for treating partial onset seizures^{10, 11}. As a mood stabilizer, LTG increases the time between episodes of depression and mania in bipolar disorder, and is particularly effective against depression^{11, 12}.

Lamotrigine and its primary metabolite, lamotrigine-2-N-glucuronide (LTG-2NG), have recently been detected in wastewater, groundwater, surface water and drinking water¹³⁻¹⁵. In surface water, LTG's detection frequency ranged from 47 to 97%¹³⁻¹⁵, and its average concentration ranged from 108 to 455 ng L⁻¹^{13, 14}. Also, in a study of the in-stream attenuation of 14 neuroactive pharmaceuticals, LTG, CBZ, and 10,11-dihydro-10,11-hydroxy-carbamazepine (DiOH-CBZ, a metabolite common to CBZ and oxcarbazepine), were determined to be most persistent, with pseudo-first order half-lives ranging from 12 to 21 h¹⁶. Limited sampling showed that LTG, CBZ and DiOH-CBZ were sequestered into stream biofilm, and the study suggested that interactions with bed sediments and stream biofilm play an important role in their fate and transport.

The predicted no-effect concentration (PNEC) of LTG in drinking water has been estimated to equal 170 µg L⁻¹ for children, based upon an exposure duration of 6 years, a drinking water ingestion rate of 1 L d⁻¹, and other factors¹⁷. This PNEC is lower and more conservative than the PNEC for adults, and orders of magnitude higher than LTG concentrations previously detected in surface and drinking waters. However, PNECs are based on available toxicological information (e.g., no observed adverse effect levels, adjusted for uncertainty factors), and the most sensitive individuals and organisms may not be discovered until after idiosyncratic reactions occur (e.g., the collapse of vulture populations exposed to diclofenac)^{18, 19}. In addition, LTG selectively blocks voltage-gated sodium channels, which predate neurons and form the basis of electrical excitability in most vertebrate and invertebrate species²⁰⁻²³. This suggests at least a potential for broad ecosystem effects. According to one study, which sought

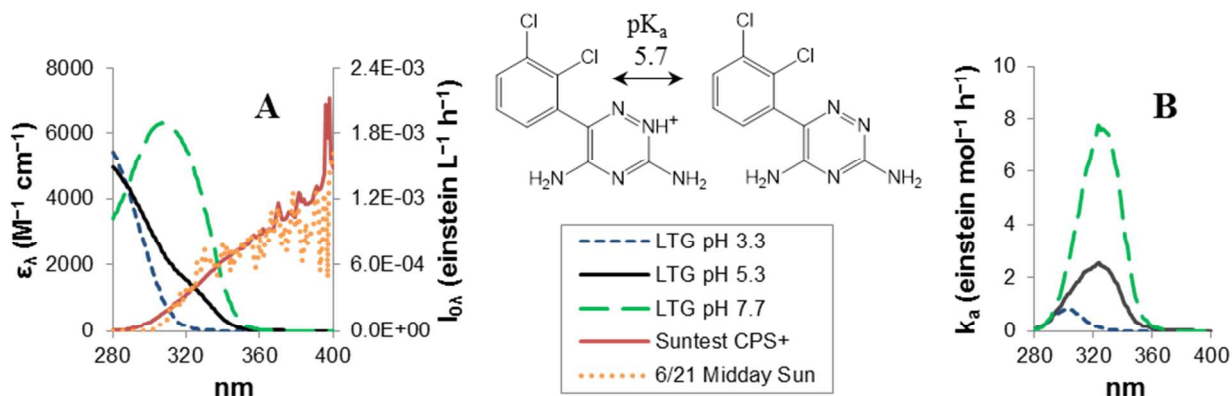


Figure 1 Molecular Structure, Absorption and Irradiance Data of Lamotrigine (LTG). Protonated and unprotonated molecular structure of LTG (center), with (A) a comparison of the spectral irradiance ($I_{0\lambda}$) of the Suntest CPS+ solar simulator, the estimated solar irradiance ($I_{0\lambda}$) in Denver, CO, USA (latitude 39.8617 °N) on June 21, 2013 at 1:00 p.m. MDT (SMARTS v 2.9.5), and LTG's molar absorptivity (ϵ_λ) in buffered aqueous solutions at pH 3.3, 5.3 and 7.7; plus (B) LTG's specific light absorption rate ($k_{a\lambda} = 2.303 \ell I_{0\lambda} \epsilon_\lambda$) in quartz glass culture tubes irradiated by the solar simulator (pathlength, ℓ , = 1 cm).

to prioritize the environmental risk of the top 200 prescription drugs from 2009, LTG was one of only 13 pharmaceuticals appearing in the top 20 for at least 6 of the 12 toxic endpoints considered²⁴.

Because LTG is incompletely removed during wastewater treatment¹⁴⁻¹⁶, and absorbs light at wavelengths present in natural waters (e.g., > 290 nm; Figure 1)²⁵, photodegradation might be expected to affect LTG's fate in sunlit waters more than biodegradation²⁶. Direct photodegradation occurs when a molecule absorbs light, becomes electronically excited, and undergoes chemical transformation. The fastest direct photochemical reactions ($\sim 10^{14} \text{ s}^{-1}$) are limited by rates of vibrational motion and electron transfer, and the slowest ($\sim 10^{-2} \text{ s}^{-1}$) are limited by slow phosphorescence rates (a competing process)²⁷. Indirect photodegradation, by comparison, is chemical transformation initiated after a co-solute (e.g., dissolved organic matter) absorbs light and becomes reactive. Various reactive species can be generated, including hydroxyl radicals ($\cdot\text{OH}$), singlet oxygen ($^1\text{O}_2$), superoxide radical ions ($\text{O}_2^{\cdot-}$), carbonate radicals ($\text{CO}_3^{\cdot-}$), and excited triplet state dissolved organic matter ($^3\text{DOM}^*$), and the fastest indirect photochemical reactions are limited by diffusion rates in water ($\sim 10^{10} \text{ M}^{-1} \text{ s}^{-1}$ at 25 °C)²⁷⁻³¹. For example, $\cdot\text{OH}$ reacts with many compounds, including natural water constituents, at nearly diffusion-controlled rates, but steady state concentrations of $\cdot\text{OH}$ in natural waters are reported to

range from only 10^{-15} to 10^{-18} M³². As a consequence, organic contaminants would generally be expected to react with $\cdot\text{OH}$ in natural waters at rates in the range of 10^{-2} to 10^{-5} h⁻¹.

Lamotrigine's direct photodegradation rate will be governed by the spectrum and intensity of available light, LTG's ability to absorb such light (i.e., molar absorptivity), and the efficiency at which the absorbed light is converted to chemical change (i.e., the reaction quantum yield). Because upper excited states rapidly decay to lowest excited singlet or triplet states, reaction quantum yields (Φ) are generally assumed to be wavelength-independent^{33, 34}. This means that reaction quantum yields can be used to predict direct photodegradation rates across different lighting conditions. Reaction quantum yields also provide the benchmark for determining the influence of indirect photodegradation, light screening, and physical quenching in natural waters³⁵. Therefore, it is appropriate to begin examining LTG's photochemical fate in sunlit waters by determining the rates, efficiency, and products of LTG's direct photodegradation.

Lamotrigine is a water soluble (0.17 mg/mL at 25 °C) weak base ($\text{pK}_a = 5.7$)³⁶. The site of LTG's protonation, and its most basic nitrogen, is located within the triazine ring where 2-N-glucuronidation occurs (Figure 1)^{36, 37}. Because the pH of most natural waters ranges from pH 6 to pH 9³⁸, LTG's neutral form will predominate, but its protonated form may also appear. pH is known to influence photochemistry because different protonation states can produce different molar absorptivities, reaction quantum yields, and photodegradation pathways³⁹⁻⁴³. Therefore, pH effects should be considered when examining LTG's direct photochemistry.

The photochemistry of LTG has not been studied in the environmental context, but LTG is known to produce a phototoxic response in some patients, and its photochemical properties have been studied on that basis⁴⁴. The mean half-life of LTG in healthy volunteers and epileptic patients receiving LTG monotherapy is 22.8 to 37.4 h⁴⁵. Accordingly, the phototoxicity study by Bilski et al. was conducted over relatively short periods (up to 1 h) with high intensity light. Among other things, the study found that irradiation of LTG produced an excited triplet state, generating $^1\text{O}_2$ and peroxidizing linoleic acid (a representative fatty acid). The study also detected chloride anions (Cl^-) by electrochemical assay, $\text{O}_2^{\cdot-}$ by spin-trapping studies, and a phenolic photoproduct resulting from dechlorination and hydroxylation of LTG's dichlorophenyl

ring. Based on these results, the study suggested that $O_2^{\cdot-}$ was formed by electron transfer from LTG to molecular oxygen, and that aryl radicals from photodechlorination might contribute to LTG's phototoxic response. Finally, the study determined that 1O_2 photosensitization is the primary mechanism for LTG phototoxicity.

The purpose of this study was to examine the direct photodegradation of LTG in waters exposed to simulated sunlight under different pH conditions, and over time periods appropriate for environmental fate analysis. The results of this study will provide a benchmark for determining the influence of indirect photodegradation, light screening, and physical quenching in natural waters, and help in predicting photodegradation pathways for LTG and similarly structured pharmaceuticals in surface waters. The results of this study will also help in prioritizing research based on photostability.

EXPERIMENTAL

The following section describes materials and methods used in this study. Additional details can be found in the Supporting Information. Unless otherwise indicated, all reported confidence intervals are 95% confidence intervals based on three replicates ($n = 3$).

Kinetics and Reaction Quantum Yield Experiments

Phosphate-buffered aqueous solutions of LTG (11.4 to 12.0 mg L⁻¹) were prepared at pH 3.3 (± 0.2), pH 5.3 (± 0.4) and pH 7.7 (± 0.1). To determine LTG's reaction quantum yield in each solution, a chemical actinometer solution (1.6 mg L⁻¹ 4-nitroacetophenone, plus 0.05% v/v pyridine) was prepared in deionized water in accordance with published methods for sunlight actinometry (Supporting Information)^{25, 46}.

During each experiment, triplicate 8.5 mL samples of the LTG and chemical actinometer solutions were placed in quartz glass culture tubes (12 mm o.d. \times 100 mm), sealed with Versa Vial PTFE/silicon closures (Supelco, Bellefonte, PA, USA), and positioned at a 35° angle within a Suntest CPS+ solar simulator (Atlas Material Testing Technology LLC, Chicago, IL, USA). The solar simulator's xenon lamp was operated at 765 W m⁻² irradiance (300 to 800 nm) using a "UV special glass" filter to eliminate wavelengths below approximately 290 nm. The spectrum

of the solar simulator was measured with a Maya 2000 Pro spectrometer (Ocean Optics, Inc., Dunedin, FL, USA), and the spectral irradiance of the solar simulator (Figure 1) was estimated with the actinometer solution, assuming a fixed spectrum and applying a factor (2.2) in accordance with published methods to account for the use of cylindrical tubes (Supporting Information)²⁵. During the experiments, the solar simulator's internal temperature (18.2 ± 0.3 °C, $n = 20$) was regulated by a Fuji Electric (Tokyo, Japan) PXZ-4 temperature controller (model SR1) and Emerson Quiet Kool (Model 6JC63) air conditioning system. For dark controls, 8.5 mL samples of the LTG and the chemical actinometer solutions were placed in borosilicate glass culture tubes (13 mm o.d. \times 100 mm), sealed with PTFE-lined screw caps, covered with aluminum foil, and positioned within the solar simulator. A 100 μ L sample was collected daily from each culture tube over either a 4 d (pH 3.3) or 5 d (pH 5.3 and 7.7) continuous exposure period, and stored at 4 °C in 2 mL amber glass vials until analysis.

LTG was quantified using an Agilent 1200 series HPLC system equipped with a UV-diode array detector (HPLC-UV; Agilent Technologies, Inc., Santa Clara, CA, USA). The chromatographic method used a Kinetex PFP column (100 \times 3.1 mm i.d., 2.6 μ m particle size, Phenomenex, Torrance, CA), maintained at 40 °C, a constant flow rate of 500 μ L min⁻¹, and the following binary gradient: 10% (A) deionized water with 5 mM ammonium acetate and 0.1% v/v formic acid, and 90% (B) acetonitrile, for 4 min; increased to 65% B over 5.5 minutes; stepped to 100% B and held for 4 minutes to flush the column; and equilibrated at 10% B for 4.5 minutes. The injection volume of each sample was 10 μ L, and the samples were quantified at 260 nm using a seven-point external calibration curve (method detection limit < 0.1 mg L⁻¹).

4-nitroacetophenone (PNAP) was also quantified using the Agilent HPLC-UV system. The chromatographic method used an XSelect CSH C₁₈ XP column (75 \times 4.6 mm i.d.; 2.5 μ m particle size; Waters Corporation, Taunton, MA, USA), maintained at 40 °C, and the following binary gradient: (A) 60% deionized water, and (B) 40% acetonitrile, at the beginning; increased to 90% B over 5 minutes at 600 μ L min⁻¹; stepped to 100% B and held for 1.5 minutes at 750 μ L min⁻¹ to flush the column; and equilibrated at 40% B for 4 minutes at 600 μ L min⁻¹. The injection volume of each sample was 10 μ L, and the samples were quantified at 270 nm using a

seven-point external calibration curve (method detection limit $< 0.1 \text{ mg L}^{-1}$). Agilent ChemStation for LC 3D Systems software was used for all LC-UV data processing.

Photoproduct Experiments

To determine LTG's photoproducts, an 8.5 mL sample of the LTG solution at pH 5.3 was irradiated according to the procedures described for the kinetics and reaction quantum yield experiments. The pH 5.3 solution was chosen for the photoproduct analysis because it contained protonated and neutral LTG and was expected to generate photoproducts from both protonation states. A 500 μL sample was collected every fourth day from each culture tube over a 12 d continuous exposure period, and a 150 μL sample was collected every fourth day thereafter until the total continuous exposure period was 24 days. The photoproduct samples were stored at 4 $^{\circ}\text{C}$ in 2 mL amber glass vials until analysis.

LTG's photoproducts were analyzed by liquid chromatography-time of flight mass spectrometry (LC-TOF MS) using an Agilent 1100 series HPLC and Agilent G3250AA MSD TOF system. The chromatographic method was identical to the chromatographic method used to quantify LTG for the kinetics and reaction quantum yield experiments. The mass spectrometer was operated in positive ion mode under the following parameters: 4000 V capillary voltage; 190 V fragmentor voltage; 45 V skimmer voltage; 300 Vpp Oct 1 RF; 45 psig nebulizer pressure; 10 L min^{-1} drying gas (nitrogen) flow; and 325 $^{\circ}\text{C}$ drying gas temperature. The injection volume of each sample was 10 or 50 μL , and internal references masses (purine, $\text{C}_5\text{H}_4\text{N}_4$, m/z 121.05087; and hexakis(1H,1H,3H-tetrafluoropropoxy)phosphazine, $\text{C}_{18}\text{H}_{18}\text{F}_{24}\text{N}_3\text{O}_6\text{P}_3$, m/z 922.00980) were infused during each chromatographic run to permit recalibration of extracted mass spectra. Agilent MassHunter Workstation Qualitative Analysis software was used for all LC-TOF MS data processing.

RESULTS

Direct Photodegradation Rates and Reaction Quantum Yields

The following section describes results from experiments in the solar simulator to determine LTG's direct photodegradation rates and reaction quantum yields in buffered aqueous solutions at pH 3.3 ± 0.2 (99 to 100% protonated), pH 5.3 ± 0.4 (50 to 86% protonated), and pH 7.7 ± 0.1

Table 1 Direct photodegradation of lamotrigine (LTG). Pseudo-first order degradation rate constants (k), half-lives ($t_{1/2}$), integrated specific light absorption rates ($\sum k_{a\lambda}$), and reaction quantum yields (Φ), with 95% confidence intervals ($\alpha = 0.05$), of buffered aqueous solutions of LTG (11.4 to 12.0 mg L⁻¹) after 4 d (pH 3.3) or 5 d (pH 5.3 and 7.7) of continuous irradiation in the solar simulator ($n = 3$), together with their estimated half-lives at latitude 40°N during summer in a flat water body at a shallow depth (i.e., < 5% attenuation).

pH	k (h ⁻¹)	$t_{1/2}$ (h)	$\sum k_{a\lambda}$ (einstein mol ⁻¹ h ⁻¹)	Φ (mol Einstein ⁻¹) [†]	predicted $t_{1/2}$ (h), summer 40°N ^{b‡}
3.3 ± 0.2	7.0 ± 0.2 × 10 ⁻³	100 ± 3	22	33 ± 2 × 10 ⁻⁵	500 ± 20
5.3 ± 0.4	6.2 ± 0.1 × 10 ⁻³	112 ± 2	99	6.3 ± 0.1 × 10 ⁻⁵	273 ± 5
7.7 ± 0.1	6.7 ± 0.2 × 10 ⁻³	103 ± 2	270	2.51 ± 0.07 × 10 ⁻⁵	230 ± 6

[†] 4-Nitroacetophenone (1.6 mg L⁻¹, 0.05% v/v pyridine) was used as a chemical actinometer, and approximately 83% was removed after 5 d (Supporting Information). [‡] Based on estimated solar irradiance in Denver, CO, USA (latitude 39.8617 °N) on June 21, 2013 at 1:00 p.m. MDT (SMARTS v 2.9.5).

(0.79 to 1.2% protonated). These pH values were chosen to represent LTG in its neutral, protonated, and partially dissociated forms, in order to examine the influence of pH on LTG's direct photodegradation.

Figure 1.A compares the spectral irradiance of the solar simulator, the estimated midday, midsummer solar irradiance in Denver, CO, USA (latitude 39.8617 °N; SMARTS v 2.9.5), and the molar absorptivities of the three buffered aqueous LTG solutions (pH 3.3, 5.3 and 7.7). Due to protonation of LTG's triazine ring, the absorption maximum of LTG's longest wavelength absorption band shifted from 307 nm (pH 7.7) to 267 nm (pH 3.3). As a consequence, in quartz glass culture tubes irradiated by the solar simulator, the specific light absorption rate (einstein mol⁻¹ h⁻¹) of LTG's neutral form (LTG⁰) was approximately 12 times greater than its protonated form (LTG⁺) (Figure 1.B). This difference increased to approximately 28 times in the estimated midday, midsummer Denver sun produced by a spectral radiation model (SMARTS v 2.9.5)⁴⁷, primarily because the estimated Denver sunlight did not include the shortest wavelengths in the solar simulator, where LTG⁺ absorbed more light (Figure 1.A; Figure SI-2, Supporting Information).

Table 1 contains the direct photodegradation rates, half-lives, and reaction quantum yields of the LTG solutions after 4 d (pH 3.3) or 5 d (pH 5.3 and 7.7) of continuous irradiation in the solar simulator. Except for one data point (pH 3.3 at 172.7 h), no dark control sample concentration was significantly different ($\alpha = 0.05$, $n = 4$) from the mean starting concentration, and the remaining data point was 96.8% of the mean starting concentration. There was no significant difference between the direct photodegradation rates of LTG^0 and LTG^+ , even though LTG^0 absorbed approximately 12 times more simulated sunlight. As reflected in LTG's reaction quantum yields at pH 3.3 and pH 7.7 (Table 1), LTG^+ converted the absorbed light to photochemical reactions approximately 13 times more efficiently than LTG^0 , offsetting the difference in their light absorption rates. When the same reaction quantum yields were used to predict LTG's half-life in a flat water body at a shallow depth (i.e., < 5% attenuation)⁴⁸ exposed to the estimated midday, midsummer Denver sun, LTG^0 was estimated to degrade more than twice as fast as LTG^+ (Table 1), primarily because LTG^0 was estimated to absorb approximately 28 times more Denver sunlight.

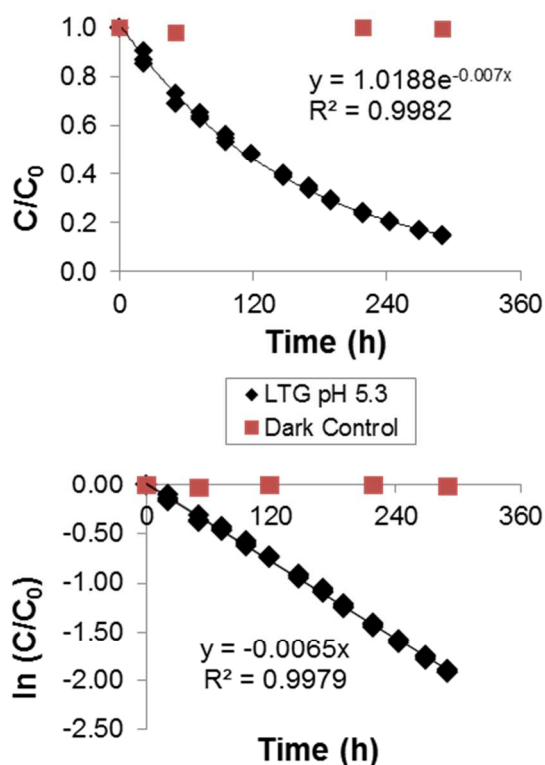


Figure 2 Photochemical loss of lamotrigine (LTG). Progress of photochemical loss of LTG in the buffered aqueous solution at pH 5.3 during 12 d (290.6 h) of continuous irradiation in the solar simulator ($n = 3$), with dark control ($n = 1$).

Figure 2 shows the photochemical loss of lamotrigine at pH 5.3 after 12 d (290.6 h) of continuous irradiation in the solar simulator. After 12 d, LTG's half-life (105 ± 2) was slightly, but significantly, shorter than the value reported in Table 1 after 5 d of continuous irradiation (112 ± 2). Close inspection of Figure 2.B reveals that LTG's photodegradation rate increased slightly with time (and decreasing LTG concentration), suggesting that some amount of self-screening occurred at the LTG concentration employed (11.7 mg L^{-1}). The reaction quantum yield, integrated specific light absorption rate, and predicted half-life calculations in Table 1

were adjusted in accordance with published methods to account for this self-screening effect (Supporting Information)^{28, 35, 46}.

In summary, LTG's direct photodegradation half-life varied little (100 ± 3 to 112 ± 2) in the solar simulator as the solution pH changed. However, LTG's molar absorptivities and reaction quantum yields at pH 3.3 and 7.7 were significantly different (Table 1), and LTG was estimated to degrade more than twice as fast at pH 7.7 under different lighting conditions. The disparity in reaction quantum yields may suggest that LTG^0 and LTG^+ are following different photodegradation pathways, and possibly producing different photoproducts. Alternatively, LTG's protonation state may influence the relaxation or energy transfer possibilities available to excited state LTG, leading to a lower quantum yield for LTG^0 .

Photoproducts

The following section describes results from experiments to determine whether LTG produced different photoproducts at different pH. HPLC-UV was utilized to detect photoproduct differences, and LC-TOF MS was used to generate accurate mass-to-charge (m/z) measurements and isotopic information to identify the resulting photoproducts.

Figure 3 contains overlapping LC-UV chromatograms for the LTG solutions at pH 3.3, 5.3, and 7.7 after 8 d of continuous irradiation in the solar simulator. Except for LTG, none of the exhibited peaks was present in any unexposed LTG solution (pre-exposure or dark control). Figure 3 is supplemented by Table 2, which contains LC-TOF MS data from the pH 5.3 solution for the numbered peaks in Figure 3. Preliminary LC-TOF MS experiments for LTG solutions at \sim pH 3 and \sim pH 8 confirmed that the proposed formulas in Table 2 also apply to the numbered peaks in Figure 3 from the pH 3.3 and pH 7.7 solutions (data not shown).

Several things stand out in Figure 3. First, many photoproducts were detected, compared to the phototoxicity study by Bilski et al., where one photoproduct was detected over shorter timeframes (up to 1 h)⁴⁴. Second, the initial concentrations of LTG in the pH 3.3, 5.3 and 7.7 solutions were similar (11.4 to 12.0 mg L^{-1}), and the peak area of LTG (peak 6) was approximately the same in all three chromatograms, indicating similar direct photodegradation

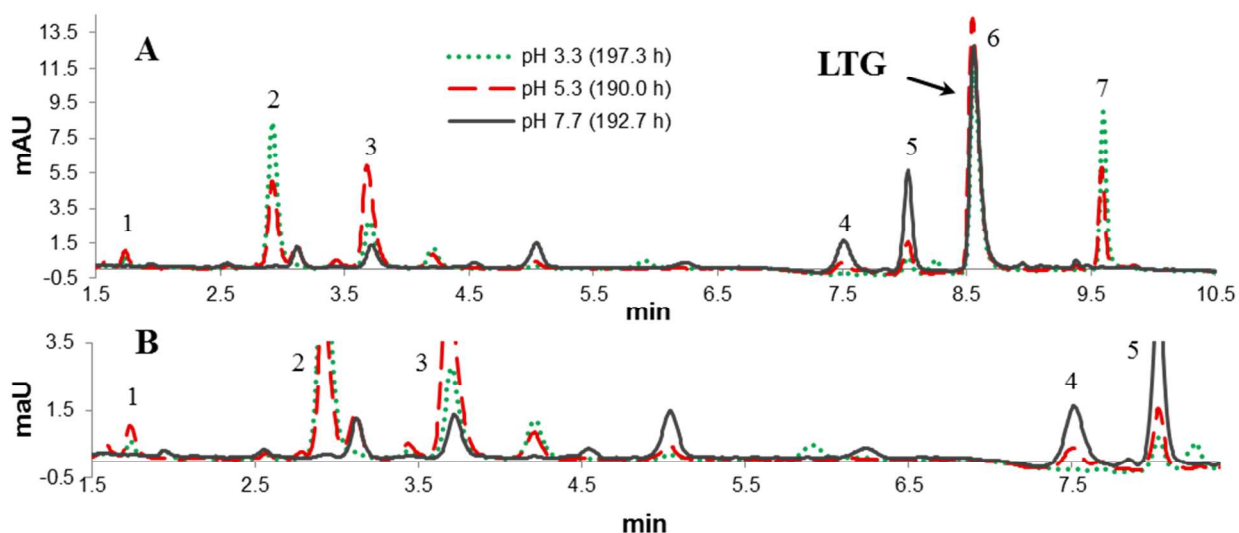


Figure 3 HPLC-UV chromatograms of lamotrigine (LTG) and its photoproducts. (A) HPLC-UV chromatograms (260 nm) of buffered aqueous solutions of LTG at pH 3.3, 5.3 and 7.7 after 8 d (192 h) of continuous irradiation in the solar simulator. The bottom panel (B) shows a portion (1.5 to 8.4 min) of the top panel (A) in greater detail. This figure is supplemented by Table 2, which provides liquid chromatography-time of flight mass spectrometry data for the numbered peaks.

rates (Table 1), and suggesting that differences in photoproduct peak areas (e.g., peak 3) were primarily the result of pH differences. Finally, some photoproduct peaks (e.g., peaks 1, 2 and 7) appeared only in solutions containing LTG^+ , and other photoproduct peaks (e.g., peak 4) appeared only in solutions containing LTG^0 .

According to the LC-TOF MS data in Table 2, peak 1 ($\text{C}_9\text{H}_8\text{ClN}_5\text{O}$) corresponds to the photoproduct detected in the phototoxicity study by Bilski et al.⁴⁴, a phenolic photoproduct resulting from dechlorination and hydroxylation of the dichlorophenyl ring of LTG ($\text{C}_9\text{H}_7\text{Cl}_2\text{N}_5$). Peak 2 ($\text{C}_9\text{H}_9\text{Cl}_2\text{N}_5\text{O}$) and peak 3 ($\text{C}_9\text{H}_8\text{Cl}_2\text{N}_4\text{O}$), by comparison, evidence reactions involving oxygen addition without dechlorination. The proposed molecular formula of peak 2 suggests a photohydration product, and the proposed molecular formula of peak 3 demonstrates that LTG lost one nitrogen and gained one hydrogen atom. Because peak 3 evidences a net increase in hydrogen atoms, peak 3 does not suggest a photoproduct resulting merely from deamination and hydroxylation of LTG's diamino-triazine ring.

Table 2 Proposed lamotrigine photoproduct identities. Liquid chromatography-time of flight mass spectrometry data for the numbered peaks in Figure 3 from the buffered aqueous solution of lamotrigine (11.7 mg L^{-1}) at pH 5.3 after 8 d (190.0 h) of continuous irradiation in the solar simulator.

peak	proposed formula (M)	m/z	ion species	absolute mass error (ppm)	double bond equivalent (DBE)
1	$\text{C}_9\text{H}_8\text{ClN}_5\text{O}$	238.04901	$[\text{M}+\text{H}]^+$	1.00	8
2	$\text{C}_9\text{H}_9\text{Cl}_2\text{N}_5\text{O}$	274.02569	$[\text{M}+\text{H}]^+$	1.02	7
3	$\text{C}_9\text{H}_8\text{Cl}_2\text{N}_4\text{O}$	259.01479	$[\text{M}+\text{H}]^+$	0.15	7
4	$\text{C}_9\text{H}_6\text{ClN}_5$	220.03845	$[\text{M}+\text{H}]^+$	0.07	9
5	$\text{C}_9\text{H}_7\text{Cl}_2\text{N}_5$	256.01513	$[\text{M}+\text{H}]^+$	0.02	8
6	$\text{C}_9\text{H}_7\text{Cl}_2\text{N}_5$	256.01513	$[\text{M}+\text{H}]^+$	0.45	8
7	$\text{C}_9\text{H}_5\text{Cl}_2\text{N}_5$	253.99948	$[\text{M}+\text{H}]^+$	0.38	9

The proposed molecular formula for peak 4 ($\text{C}_9\text{H}_6\text{ClN}_5$), which appeared only in solutions containing LTG^0 , indicates that LTG lost HCl, and added one double bond equivalent (DBE 8 \rightarrow 9). Given the aromatic structure of LTG's dichlorophenyl and triazine rings, this suggests a photocycloaddition reaction, and the formation of a third ring. Therefore, peak 4 was tentatively assigned the one chlorine-tricyclic structure in Figure 4.

The proposed molecular formula for peak 5 ($\text{C}_9\text{H}_7\text{Cl}_2\text{N}_5$) indicates an LTG isomer. Peak 5 was not present at 0 d, and increased in size after 4, 8 and 12 d of continuous irradiation in the solar simulator (Figure SI-3), conclusively establishing that peak 5 is an LTG photoproduct, and not the result of poor chromatography.

Finally, the proposed molecular formula for peak 7 ($\text{C}_9\text{H}_5\text{Cl}_2\text{N}_5$), which appeared only in solutions containing LTG^+ , indicates that LTG lost H_2 , and added one double bond equivalent (DBE 8 \rightarrow 9). In accordance with the reasoning for peak 4, peak 7 was tentatively assigned the two chlorine-tricyclic structure in Figure 4.

Figure 5 shows changes in the areas of the numbered peaks in Figure 3 over a 28 d (670.9 h) extended irradiation period in the solar simulator. Approximately 90% of the initial LTG concentration was eliminated after 12 d (290.2 h). Thereafter, the areas of peaks 2 and 3 declined sharply, the areas of peaks 1 and 4 declined slowly, and the areas of peaks 5 and 7 were relatively stable. There was no relationship between photoproduct stability and pH, because

peak 4 only appeared in solutions containing LTG^0 , peak 5 appeared at every pH, and peak 7 only appeared in solutions containing LTG^+ . According to Figure 5, peaks 4, 5 and 7 were somewhat to very stable over the 16 d period after most of the initial LTG concentration had been eliminated, suggesting that the associated photoproducts were even more stable than LTG under simulated sunlight.

In summary, several photoproducts were detected, and their identities, relative abundances and reaction mechanisms were influenced by solution pH. Molecular formulas were proposed for the most prominent peaks, and molecular structures were proposed for peak 4, which appeared only in solutions containing LTG^0 , and peak 7, which appeared only in solutions containing LTG^+ . Three of the most prominent peaks appeared to be even more stable than LTG in simulated sunlight, but no relationship between solution pH and photostability was observed.

DISCUSSION

Direct Photodegradation Rates and Reaction Quantum Yields

According to Table 1, LTG's reaction quantum yield was 13 times higher at pH 3.3, when LTG was almost 100% protonated, than at pH 7.7, when LTG was approximately 1% protonated. However, LTG^+ absorbs less light than LTG^0 at wavelengths present in natural waters. Therefore, pH influenced LTG's direct photodegradation rate *both* by influencing LTG's ability to absorb the available light, and by influencing the efficiency at which such light is converted to photochemical reactions. Because LTG's neutral form is expected to predominate in natural waters, the photochemistry of LTG^0 is expected to exert a greater influence on LTG's fate in sunlit waters.

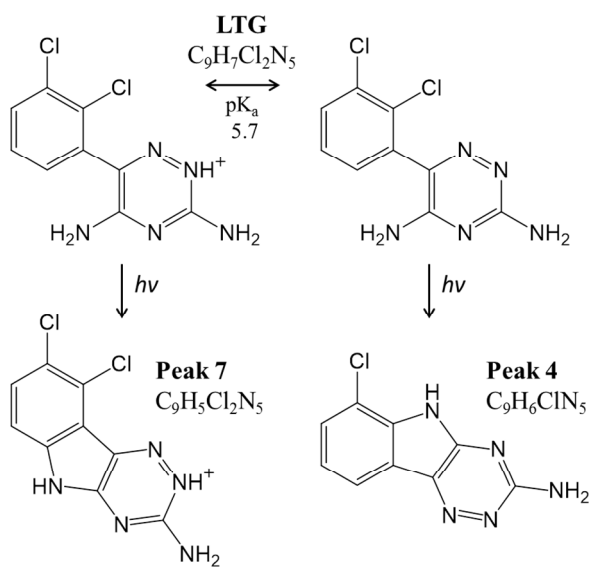


Figure 4 Selected photoproduct structures. Proposed structures for photoproduct peaks 4 and 7 in Figure 3, arising from irradiation of the buffered aqueous solution of lamotrigine (LTG, 11.7 mg L^{-1}) at pH 5.3.

LTG's reaction quantum yield at pH 5.3 arguably should have been closer to that of pH 3.3 (almost 100% protonated) than that of pH 7.7 (approximately 1% protonated), because LTG is 72% protonated at pH 5.3. In general, when a molecule is present in more than one protonation state, its photochemistry is expected to reflect the photochemistry of all available protonation states in an integrative manner^{39, 49}. In fact, LTG's molar absorptivity at pH 5.3 did more closely resemble that of pH 3.3 (Figure 1.A). Chlorinated arenes (like LTG's dichlorophenyl ring) have been observed to undergo photochemical reactions through excited state charge transfer complexes⁵⁰, and there is at least some potential for LTG⁰ and LTG⁺ to form ground state complexes via cation- π bond interactions⁵¹, but the LTG concentrations used in this study are low (< 0.05 mM), and LTG concentrations in the environment are even lower. It is more likely that the reaction quantum yields in Table 1 are affected by small errors in determining the solar simulator's spectral irradiance or LTG's molar absorptivity, particularly at pH 3.3 and 5.3 where their spectral overlap is small (Figure 1). Such errors can cause significant differences in reaction quantum yields⁴⁰.

In this study, LTG's reaction quantum yields ranged from 2.51×10^{-5} (pH 7.7) to 33×10^{-5} (pH 3.3) mol einstein⁻¹. These are similar to reaction quantum yields reported for CBZ, which have ranged from 6×10^{-5} to 1.3×10^{-4} mol einstein⁻¹^{29, 52-57}. Many pharmaceuticals undergo direct photodegradation with greater efficiency than CBZ and LTG (e.g., naproxen, $\Phi = 0.012$; diclofenac: $\Phi = 0.094$ to 0.13; and sulfamethoxazole, $\Phi = 0.028$ to 0.959 from pH 9.2 to pH 3.2)^{26, 40}, which might explain why CBZ and LTG seem more recalcitrant than many other drugs in surface waters. However, indirect photodegradation is significantly faster and more efficient than direct photodegradation in some pharmaceuticals⁵⁸⁻⁶⁰, and further study is needed to examine the effect of indirect photochemistry and biodegradation on LTG's fate in sunlit waters. For example, LTG

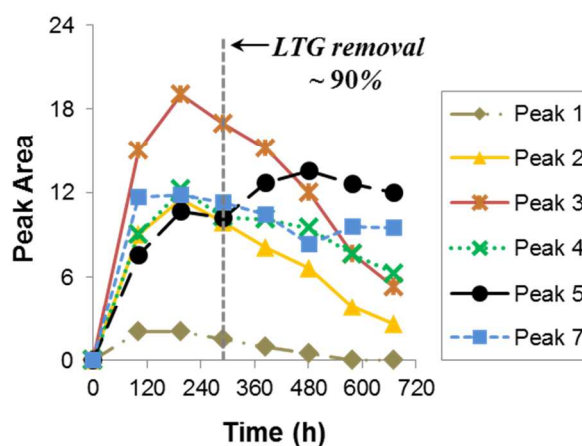


Figure 5 Lamotrigine (LTG) photoproducts. Peak areas (detection wavelength = 260 nm) for the numbered peaks in Figure 3 over a 28 d (670.9 h) extended irradiation period ($n = 1$).

produces an excited triplet state upon photoexcitation⁴⁴, which suggests the possibility of triplet energy transfer to dissolved organic matter (DOM)⁶¹, or triplet state energy transfer from $^3\text{DOM}^*$ ²⁸. Similarly, excited state LTG has been reported to undergo electron transfer reactions⁴⁴, which suggests the possibility of electron transfer reactions with DOM, $\text{CO}_3^{\bullet-}$, and other natural water constituents^{31, 62, 63}. The relative importance of each reactant will depend on its steady-state concentration and second-order rate constant for reaction with LTG³¹, but LTG's direct photodegradation rates (Table 1) do appear consistent with the range of reaction rates described in the Introduction for reactions between organic contaminants and $\cdot\text{OH}$.

Photoproducts

As Figure 3 demonstrates, pH and degree of protonation affected the identities and relative abundances of most LTG photoproducts. For example, peaks 1, 2 and 7 appeared only in solutions containing LTG^+ , and peak 4 appeared only in solutions containing LTG^0 .

Figure 4 contains proposed molecular structures for peaks 4 and 7, both of which involve the photochemical addition of an amino group from LTG's triazine ring to the adjacent dichlorophenyl ring. In the case of peak 4, dechlorination also occurred. The resulting photoproducts feature tricyclic heteroaromatic systems, and Figure 5 suggests that both photoproducts are more stable than LTG in simulated sunlight. Given the apparent similarity of the peak 4 and 7 photoproducts, their mutual exclusivity at different pH is surprising, and suggests that different photodegradation pathways were involved.

Peaks 1 and 7 both evidence the addition of an electron-donating group (OH^- or R-NH_2) to LTG's dichlorophenyl ring. In the case of peak 1, dechlorination also occurred. Each peak appeared only in solutions containing LTG^+ , suggesting a similar reaction mechanism. Because the positive charge in LTG^+ is located on the triazine ring, one possibility is that photoexcitation and intersystem crossing to LTG^{+*} 's excited triplet state caused the transfer of an electron from LTG^{+*} 's dichlorophenyl ring to its triazine ring, facilitating the addition of electron-donating groups to LTG^{+*} 's dichlorophenyl ring (Figure SI-4, Supporting Information). Bilski et al. demonstrated that excited triplet state LTG forms upon irradiation⁴⁴, and addition reactions have been reported to occur at aromatic rings activated by single-electron oxidation⁶⁴ or electron

withdrawing groups⁶⁵. Alternatively, LTG⁺'s protonated triazine ring might be directing photosubstitution reactions to adjacent (ortho) positions on the dichlorophenyl ring⁶⁶, but this mechanism might also be expected to produce the peak 4 photoproduct, which does not appear in solutions containing LTG⁺. More work is needed to elucidate the mechanisms involved, and the results of such reactions in the presence of natural water constituents like DOM. However, it is significant that the peak 7 photoproduct forms without dechlorination, a common process among other chlorinated arenes⁶⁷⁻⁷⁰.

Peak 4 appears to evidence electron transfer in the opposite direction, possibly due to the change in LTG's protonation state. Specifically, peak 4 appears to evidence the transfer of an electron from the 5-amino group in LTG's triazine ring to its dichlorophenyl ring, causing dechlorination, and the formation of a new pyrrole ring (Figure SI-5, Supporting Information). Triclosan has been observed to undergo a similar reaction, resulting in the formation of a 1,4-dioxin ring^{41, 71, 72}. In addition, Bilski et al. observed O₂^{•-} formation by electron transfer from LTG to molecular oxygen, and "strongly" accelerated Cl⁻ production in the presence of ascorbic acid (a reducing agent⁷³) during LTG photodegradation in polar solvents⁴⁴. Finally, protonation of the electron-donating amino group in 4-chloroaniline has been shown to inhibit heterolytic photodechlorination⁶⁹, and protonation of LTG's triazine ring did inhibit the formation of photoproduct peak 4 in this study. Additional work is needed to elucidate the mechanisms involved, and to explore the effect of such reactions in natural waters, where reducing agents comparable to ascorbic acid (e.g., redox active chromophores in DOM³⁰) might enhance LTG's photodegradation through similar electron transfer reactions.

The results of this study suggest that photoinduced substitution and electron transfer reactions could be important pH-influenced photodegradation pathways in natural waters, particularly for LTG and similarly structured pharmaceuticals. Because LTG's neutral form will predominate in natural waters, the electron transfer process could be especially important.

CONCLUSION

To our knowledge, this is the first study to examine the direct photodegradation of LTG under environmentally relevant conditions, even though LTG has been detected in surface waters at

frequencies of 47 to 97%¹³⁻¹⁵, found to be relatively persistent among 14 neuroactive pharmaceuticals during in-stream attenuation¹⁶, and ranked highly across all toxicity endpoints when comparing the environmental risks of top-selling prescription drugs²⁴. Three general findings from this study have special significance.

First, LTG undergoes direct photodegradation slowly and inefficiently under environmentally relevant conditions. Under the estimated midday, midsummer sun in Denver, CO, USA (latitude 39.8617 °N; SMARTS v 2.9.5), LTG's half-life was estimated to equal at least 230 ± 6 h of continuous sunlight, and LTG's reaction quantum yield was determined to be no greater than 3.3×10^{-4} mol einstein⁻¹. The reaction quantum yield of CBZ is similar ($\Phi \leq 1.3 \times 10^{-4}$ mol einstein⁻¹)^{29, 52-57}, and CBZ has been described as the most frequently detected and studied compound in North America and Europe, and third in Asia¹. Little is known about the biodegradation and indirect photodegradation of LTG in natural waters, but the existing data suggest that LTG is approximately as recalcitrant as CBZ, and commonly present in surface waters like other pharmaceuticals in its therapeutic class.

Second, LTG appears in neutral and protonated forms in natural waters, and this has a significant effect on the direct photodegradation of LTG. Lamotrigine's specific light absorption rate was 12 times higher, and its reaction quantum yield was 13 times lower, at pH 7.7 versus pH 3.3. In addition, certain photoproducts appeared only when neutral LTG was present, and others appeared only when protonated LTG was present. This mutually exclusive behavior suggested different reaction mechanisms, even for photoproducts that appeared structurally similar.

Finally, the pH-dependent reactions observed in this study may be important to LTG's photodegradation in natural waters, and to the photodegradation of structurally similar compounds. Lamotrigine's pH-dependent reactions suggested a potential for accelerated LTG photodegradation through photoinduced substitution reactions with π electron donors present in DOM, and photoinduced electron transfer reactions with redox active chromophores in DOM. These reactions are not novel⁶³, but they are not often considered as alternatives to photosensitization and reactive intermediate species (e.g., $\cdot\text{OH}$, $^1\text{O}_2$, and $\text{O}_2^{\cdot-}$) in natural waters.

This study was intended to provide insight into the photodegradation of LTG and similarly structured compounds in natural waters. The results of this study will provide a benchmark for determining the influence of indirect photodegradation, light screening, and physical quenching on LTG's photodegradation, and might also help in prioritizing research based on photostability in natural waters.

ASSOCIATED CONTENT

Supporting Information

Detailed descriptions of chemicals, solutions, analytical methods, and chemical actinometry procedures; comparison of LTG's specific light absorption rate in simulated and estimated sunlight; extracted ion chromatograms for LTG and its photoisomer over time; and proposed photodegradation pathways to peaks 4 and 7.

AUTHOR INFORMATION

Corresponding Author

*Phone: 970-491-6235; e-mail: borch@colostate.edu

Notes

The authors declare no competing financial interest.

ACKNOWLEDGMENTS

This research was primarily supported by the United States – Israel Binational Agricultural Research and Development Fund (US-4551-12). In addition, A.L. received travel, salary and other support as a visiting scientist from the National Natural Science Foundation of China (NSFC) (NO.41001145), Projects of International Cooperation and Exchanges NSFC (41210104050), the international visiting project of Young Teachers in universities of Shandong Province, China, and the Foundation of Shandong University of Technology (NO.4072). We would like to thank Jessica G. Davis and Heather N. Storteboom of the Colorado State University Department of Soil and Crop Sciences, Greg P. Dooley, Brian K. Cranmer and Jana C. Jokerst of the Colorado State University Center for Environmental Medicine, E. Michael Thurman and Imma Ferrer of the University of Colorado at Boulder Center for Environmental

Mass Spectrometry, and Karl G. Linden and Sara Beck of the University of Colorado at Boulder Civil, Environmental, and Architectural Engineering Department, for their technical support or assistance.

REFERENCES

1. S. R. Hughes, P. Kay and L. E. Brown, *Environmental Science & Technology*, 2012, **47**, 661-677.
2. M. J. Benotti, R. A. Trenholm, B. J. Vanderford, J. C. Holady, B. D. Stanford and S. A. Snyder, *Environmental Science & Technology*, 2009, **43**, 597-603.
3. E. Vulliet and C. Cren-Olivé, *Environmental Pollution*, 2011, **159**, 2929-2934.
4. B. Huerta, S. Rodriguez-Mozaz and D. Barcelo, *Analytical and Bioanalytical Chemistry*, 2012, **404**, 2611-2624.
5. IMS Health Incorporated, *Top Therapeutic Classes by U.S. Dispensed Prescriptions (2011)*, http://www.imshealth.com/deployedfiles/ims/Global/Content/Corporate/Press%20Room/Top-Line%20Market%20Data%20&%20Trends/2011%20Top-line%20Market%20Data/Top_Therapy_Classes_by_RX.pdf, Accessed October 23, 2013.
6. IMS Health Incorporated, *Top 20 Global Therapeutic Classes, 2011, Total Audited Markets*, http://www.imshealth.com/deployedfiles/ims/Global/Content/Corporate/Press%20Room/Top-Line%20Market%20Data%20&%20Trends/2011%20Top-line%20Market%20Data/Top_20_Global_Therapeutic_Classes.pdf, Accessed October 23, 2013.
7. E. Vulliet, C. Cren-Olivé and M.-F. Grenier-Loustalot, *Environmental Chemistry Letters*, 2011, **9**, 103-114.
8. M. Huerta-Fontela, M. Teresa Galceran and F. Ventura, *Water Research*, 2011, **45**, 1432-1442.
9. Drugs.com, *Top 200 Drugs for 2008 by Sales*, http://www.drugs.com/top200_2008.html, Accessed October 23, 2013.
10. F. Gaeta, C. Alonzi, R. L. Valluzzi, M. Viola, M. Elia and A. Romano, *Current Pharmaceutical Design*, 2008, **14**, 2874-2882.
11. F. J. E. Vajda, S. Dodd and D. Horgan, *Journal of Clinical Neuroscience*, 2013, **20**, 13-16.
12. D. R. Goldsmith, A. J. Wagstaff, T. Ibbotson and C. M. Perry, *Drugs*, 2003, **63**, 2029-2050.
13. I. Ferrer and E. M. Thurman, *Journal of Chromatography A*, 2012.
14. I. Ferrer and E. M. Thurman, *Analytical Chemistry*, 2010, **82**, 8161-8168.
15. J. H. Writer, I. Ferrer, L. B. Barber and E. M. Thurman, *Science of The Total Environment*, 2013, **461-462**, 519-527.
16. J. H. Writer, R. C. Antweiler, I. Ferrer, J. N. Ryan and E. M. Thurman, *Environmental Science & Technology*, 2013, **47**, 9781-9790.
17. V. L. Cunningham, S. P. Binks and M. J. Olson, *Regulatory Toxicology and Pharmacology*, 2009, **53**, 39-45.

18. J. L. Walgren, M. D. Mitchell and D. C. Thompson, *Critical Reviews in Toxicology*, 2005, **35**, 325-361.
19. J. L. Oaks, M. Gilbert, M. Z. Virani, R. T. Watson, C. U. Meteyer, B. A. Rideout, H. L. Shivaprasad, S. Ahmed, M. J. I. Chaudhry, M. Arshad, S. Mahmood, A. Ali and A. A. Khan, *Nature*, 2004, **427**, 630-633.
20. A. L. Goldin, *Journal of Experimental Biology*, 2002, **205**, 575-584.
21. H. H. Zakon, *Proceedings of the National Academy of Sciences of the United States of America*, 2012, **109**, 10619-10625.
22. W. Lason, M. Dudra-Jastrzebska, K. Rejdak and S. J. Czuczwar, *Pharmacological Reports*, 2011, **63**, 271-292.
23. A. Nardi, N. Damann, T. Hertrampf and A. Kless, *Chemmedchem*, 2012, **7**, 1712-1740.
24. Z. Dong, D. B. Senn, R. E. Moran and J. P. Shine, *Regulatory Toxicology and Pharmacology*, 2013, **65**, 60-67.
25. D. Dulin and T. Mill, *Environmental Science & Technology*, 1982, **16**, 815-820.
26. A. L. Boreen, W. A. Arnold and K. McNeill, *Aquatic Sciences*, 2003, **65**, 320-341.
27. N. J. Turro, V. Ramamurthy and J. C. Scaiano, *Modern molecular photochemistry of organic molecules*, University Science Books, Sausalito, 2010.
28. R. G. Zepp, P. F. Schlotzhauer and R. M. Sink, *Environmental Science & Technology*, 1985, **19**, 74-81.
29. E. De Laurentiis, S. Chiron, S. Kouras-Hadef, C. Richard, M. Minella, V. Maurino, C. Minero and D. Vione, *Environmental Science & Technology*, 2012, **46**, 8164-8173.
30. S. Garg, A. L. Rose and T. D. Waite, *Geochim. Cosmochim. Acta*, 2011, **75**, 4310-4320.
31. S. Canonica, T. Kohn, M. Mac, F. J. Real, J. Wirz and U. von Gunten, *Environmental Science & Technology*, 2005, **39**, 9182-9188.
32. J. M. Burns, W. J. Cooper, J. L. Ferry, D. W. King, B. P. DiMento, K. McNeill, C. J. Miller, W. L. Miller, B. M. Peake, S. A. Rusak, A. L. Rose and T. D. Waite, *Aquatic Sciences*, 2012, **74**, 683-734.
33. R. G. Zepp, *Environmental Science & Technology*, 1978, **12**, 327-329.
34. N. J. Turro, V. Ramamurthy, W. Cherry and W. Farneth, *Chemical Reviews*, 1978, **78**, 125-145.
35. R. B. Young, D. E. Latch, D. B. Mawhinney, T.-H. Nguyen, J. C. C. Davis and T. Borch, *Environmental Science & Technology*, 2013, **47**, 8416-8424.
36. M. L. Cheney, N. Shan, E. R. Healey, M. Hanna, L. Wojtas, M. J. Zaworotko, V. Sava, S. J. Song and J. R. Sanchez-Ramos, *Crystal Growth & Design*, 2009, **10**, 394-405.
37. R. Chadha, A. Saini, S. Khullar, D. S. Jain, S. K. Mandal and T. N. Guru Row, *Crystal Growth & Design*, 2013, **13**, 858-870.
38. W. Stumm and J. J. Morgan, *Aquatic Chemistry*, 3rd edn., John Wiley & Sons, Inc., New York, NY, USA, 1996.
39. X. X. Wei, J. W. Chen, Q. Xie, S. Y. Zhang, L. K. Ge and X. L. Qiao, *Environmental Science & Technology*, 2013, **47**, 4284-4290.
40. F. Bonvin, J. Omlin, R. Rutler, W. B. Schweizer, P. J. Alaimo, T. J. Strathmann, K. McNeill and T. Kohn, *Environmental Science & Technology*, 2013, **47**, 6746-6755.
41. C. Tixier, H. P. Singer, S. Canonica and S. R. Muller, *Environmental Science & Technology*, 2002, **36**, 3482-3489.
42. J. K. Challis, J. C. Carlson, K. J. Friesen, M. L. Hanson and C. S. Wong, *Journal of Photochemistry and Photobiology a-Chemistry*, 2013, **262**, 14-21.

43. E. Fasani, M. Rampi and A. Albini, *Journal of the Chemical Society-Perkin Transactions 2*, 1999, 1901-1907.
44. P. J. Bilski, M. A. Wolak, V. Zhang, D. E. Moore and C. F. Chignell, *Photochemistry and Photobiology*, 2009, **85**, 1327-1335.
45. B. Rambeck and P. Wolf, *Clinical Pharmacokinetics*, 1993, **25**, 433-443.
46. A. Leifer, *The kinetics of environmental aquatic photochemistry: Theory and practice*, American Chemical Society, Washington, DC, 1988.
47. C. A. Gueymard, *Sol. Energy*, 2001, **71**, 325-346.
48. R. G. Zepp and D. M. Cline, *Environmental Science & Technology*, 1977, **11**, 359-366.
49. F. E. Scully and J. Hoigne, *Chemosphere*, 1987, **16**, 681-694.
50. S. Lazzaroni, S. Protti, M. Fagnoni and A. Albini, *Journal of Photochemistry and Photobiology A-Chemistry*, 2010, **210**, 140-144.
51. J. Spöner, J. Leszczynski and P. Hobza, *Biopolymers*, 2001, **61**, 3-31.
52. H. Yamamoto, Y. Nakamura, S. Moriguchi, Y. Nakamura, Y. Honda, I. Tamura, Y. Hirata, A. Hayashi and J. Sekizawa, *Water Research*, 2009, **43**, 351-362.
53. M. W. Lam and S. A. Mabury, *Aquatic Sciences*, 2005, **67**, 177-188.
54. R. Andreozzi, M. Raffaele and P. Nicklas, *Chemosphere*, 2003, **50**, 1319-1330.
55. L. Carlos, D. O. Martire, M. C. Gonzalez, J. Gomis, A. Bernabeu, A. M. Amat and A. Arques, *Water Research*, 2012, **46**, 4732-4740.
56. S. Chiron, C. Minero and D. Vione, *Environmental Science & Technology*, 2006, **40**, 5977-5983.
57. V. J. Pereira, H. S. Weinberg, K. G. Linden and P. C. Singer, *Environmental Science & Technology*, 2007, **41**, 1682-1688.
58. J. J. Werner, K. McNeill and W. A. Arnold, *Chemosphere*, 2005, **58**, 1339-1346.
59. Y. Chen, C. Hu, X. X. Hu and J. H. Qu, *Environmental Science & Technology*, 2009, **43**, 2760-2765.
60. A. Y. C. Lin and M. Reinhard, *Environmental Toxicology and Chemistry*, 2005, **24**, 1303-1309.
61. J. Wenk, S. N. Eustis, K. McNeill and S. Canonica, *Environ Sci Technol*, 2013, **47**, 12802-12810.
62. S. Canonica, U. Jans, K. Stemmler and J. Hoigne, *Environmental Science & Technology*, 1995, **29**, 1822-1831.
63. J. Wenk, U. von Gunten and S. Canonica, *Environmental Science & Technology*, 2011, **45**, 1334-1340.
64. P. R. Tentscher, S. N. Eustis, K. McNeill and J. S. Arey, *Chemistry – A European Journal*, 2013, **19**, 11216-11223.
65. G. G. Wubbels, T. R. Brown, T. A. Babcock and K. M. Johnson, *The Journal of Organic Chemistry*, 2008, **73**, 1925-1934.
66. E. Havinga and J. Cornelisse, *Pure and Applied Chemistry*, 1976, **47**, 1-10.
67. J. Grimshaw and A. P. De Silva, *Chemical Society Reviews*, 1981, **10**, 181-203.
68. K. Othmen and P. Boule, *Journal of Photochemistry and Photobiology A: Chemistry*, 1999, **121**, 161-167.
69. B. Guizzardi, M. Mella, M. Fagnoni, M. Freccero and A. Albini, *J. Org. Chem.*, 2001, **66**, 6353-6363.
70. M. Freccero, M. Fagnoni and A. Albini, *J. Am. Chem. Soc.*, 2003, **125**, 13182-13190.

71. D. E. Latch, J. L. Packer, W. A. Arnold and K. McNeill, *Journal of Photochemistry and Photobiology A-Chemistry*, 2003, **158**, 63-66.
72. S. Kliegman, S. N. Eustis, W. A. Arnold and K. McNeill, *Environmental Science & Technology*, 2013.
73. K. Kiruthiga, P. Aravindan, S. Anandan and P. Maruthamuthu, *Research on Chemical Intermediates*, 2006, **32**, 115-135.